

Violation of the “information-disturbance relationship” in finite-time quantum measurements

A. Thilagam*

*Information Technology, Engineering and Environment,
University of South Australia, Adelaide 5095, South Australia*

The effect of measurement attributes (quantum level of precision, finite duration) on the classical and quantum correlations is analysed for a pair of qubits immersed in a common reservoir. We show that the quantum discord is enhanced as the precision of the measuring instrument is increased, and both the classical correlation and the quantum discord experience noticeable changes during finite-time measurements performed on a neighboring partition of the entangled system. The implications of these results on the “information-disturbance relationship” are examined, with critical analysis of the delicate roles played by quantum non-locality and non-Markovian dynamics in the violation of this relationship, which appears surprisingly for a range of measurement attributes. This work highlights that the fundamental limits of quantum mechanical measurements can be altered by exchanges of non-classical correlations such as the quantum discord with external sources, which has relevance for cryptographic technology.

I. INTRODUCTION

The role of measurements in quantum correlation and decoherence processes presents a challenging area of investigation of quantum systems^{1–7}. Some progress has been made in the understanding of the links between quantum measurements and decoherence processes which results in the breakdown of phases in the superposed states⁸. In the “decoherence scheme”, a quantum system which survives while in contact with an environment is guided to its pointer states⁹. The view that an open quantum system is equivalent to a system that is continuously measured by its environment has been examined using various approaches in other works^{10,11}. Some issues still remain in relation to the links between quantum correlations and non-locality. This stems from difficulties in formulating a rigorous definition for non-locality, partly due the non-objectivity-non-locality issue. In general, quantum theory presents a well-defined platform in which to investigate quantum measurements, with no apparent conflict if the notion that wave functions do collapse is excluded in favor of quantum state reduction¹².

Quantum measurements have been used in the formulation of several measures of quantum correlations, including the quantum discord^{13–15}, an entity that is known to possess more generalized properties than other well established measures such as the Wootters concurrence¹⁶. The quantum discord is useful in differentiating processes which are based on locally accessible correlations from those that incorporate generically non-classical features^{17–21}. The quantum discord of a specific system is obtained by performing a set of positive-operator-valued measurements (POVM) in a neighboring partition. At zero quantum discord, a measurement procedure allows external observers to obtain all information about a bipartite system without disturbing it.

Recently, the tradeoff between information gained due to quantum measurement and the disturbance on the observed quantity, has been examined in several works^{22–26}. One study²³ showed that an informative measurement affects at least one state of the system, and the quantity of disturbance on the state is lower bounded by the amount of information that can distinguish the input and corresponding output states. The trade-off between the magnitude of information obtained via quantum measurements and disturbance on the evolution of the system could be reinterpreted using the Heisenberg uncertainty principle^{24–26}. Heisenberg²⁷ first raised the idea that any attempt to measure the position of a particle with higher precision will result in a greater disturbance as quantified by the mean square deviations of the momentum measurements. In a recent experimental study²⁸ involving weak measurements, Heisenberg’s “measurement-disturbance relationship” was noted to be violated. In another work²⁹ involving “entanglement-enhanced measurement”, the spinning of electrons in atoms was observed without any disturbance to the atomic cloud.

This study is aimed at examining the attributes of the measurement process and imperfections which distort the quantum correlations present in entangled systems. Following the approach in an earlier work³⁰, we focus on two key attributes: a) the measurement duration, and, b) the quantum level precision for a model system of a qubit pair immersed in a common reservoir. In order to keep the numerical analysis tractable, we adopt the Feynman’s path integral framework^{31,32} to interpret quantum measurements. In particular we employ a variant of this formalism based on the restricted path integral formalism^{7,33}. Within the restricted path framework, the continuous measurement of a quantity with a given result is monitored by constraints imposed on the Feynman’s path integral. Accordingly an anti-Hermitian term is added to the Hamiltonian that describes the dynamics of the measured system. In the presence of non-Hermitian terms introduced during highly precise measurements, the measured system may evolve via one or

more complex routes, and the final readout becomes ill-defined. The key feature in this work is thus the perusal of the idea that state reduction can be associated with imperfect measurements, which departs from conventional treatments.

This paper is organized as follows. In Section II we describe the restricted path integral approach for energy measurements incorporating the non-ideal attributes of the measuring device. Description of the quantum discord measures and details of the qubit pair system under study is provided in Section III, including an analysis of the influence of critical parameters in the violation of a Bell inequality associated with the quantum state of the qubit pair. In Section IV, the effect of the measurement precision and finite time duration on the quantum correlation measure is evaluated and numerical results are presented. The information-measurement precision trade-off relations is examined in Section V and the implication of results obtained in Section IV on the “information-disturbance relationship” is discussed. In Section VI non-Markovianity as quantified by the fidelity difference is used to analyze the flow of information during quantum measurements, and the issues of quantum non-locality and non-Markovian dynamics during violation of the “information-disturbance relationship”, is examined. The conclusion is provided in Section VII.

II. THE RESTRICTED PATH INTEGRAL APPROACH FOR ENERGY MEASUREMENTS

We recall the two key elements in Feynman’s path integral formalism^{31,32}: the first involves the superposition principle which yields the transition amplitude for a given quantum process, and in the absence of measurements. Under this scheme, the probability amplitude of the transition from the initial to the final state of the system is obtained via summation of the amplitudes of all possible paths which could also interfere with each other. The second feature in Feynman’s formalism involves the weight attached to each individual paths that is included during the summation procedure. This weight provides a measure of contribution of each constituent path.

The restricted path integral is derived^{7,33–35} from the Feynman path integral through the incorporation of a weight functional within the integrand that represents the summation of all tracks linking the origin and destination point. We recall that the Feynman’s propagator, $K_{[E]}(q', \tau; q, 0)$ in the phase-space representation at time τ is given by^{31,32}

$$K(q', \tau; q, 0) = \int d[q]d[p] e^{\frac{i}{\hbar} \int_0^\tau [p\dot{q} - \hat{H}_0(q,p)] dt} \quad (1)$$

where \hat{H}_0 is the Hamiltonian of the closed (unmeasured) quantum system and $[p]$ and $[q]$ are the paths in the momentum and configuration spaces respectively. In Mensky’s formalism, the output of a measured quantum system is expressed in terms of constrained paths associated with a weight functional $w_{[E]}$ ⁷. This functional may assume a Gaussian form, with a damping magnitude that is proportional to the squared difference of the observed value along the paths and the actual measurement result. A system subjected to measurement therefore evolves via a propagator which modifies Eq.(1) according to^{35,36}

$$K_{[E]}(q', \tau; q, 0) = \int d[q]d[p] e^{\frac{i}{\hbar} \int_0^\tau [p\dot{q} - \hat{H}_0(q,p)] dt} w_{[E]} \quad (2)$$

This relation highlights the dependence of a selected measurement output such as E for a measuring instrument that incurs an error E_r during a measurement duration, τ

The sensitivity or error during measurements of the energy levels of a two-level system is known to influence inter-level transitions^{36–38}. In a recent work³⁰, singularities known as exceptional points³⁹ are shown to appear at the branch point of eigenfunctions at a critical measurement precision E_r^c . The significance of Mensky’s formalism lies in the inclusion of attributes of the measuring device that may influence the dynamics of the quantum system under observation. This has obvious implications for the evaluation of the quantum discord in quantum systems, as will be shown later in this work. The use of the Gaussian measure, $w_{[E]} = \exp\left\{-\frac{\langle(H_0 - E)^2\rangle}{\Delta E^2}\right\}$ enables the effect of the measurement to be incorporated via the effective Hamiltonian^{36,37} for a two-level system

$$\hat{H}_{eff} = \hat{H}_0 - i \frac{\hbar}{\tau E_r^2} (\hat{H}_0 - E)^2 \quad (3)$$

where $\langle \dots \rangle$ denotes the time-average for the duration τ during which measurement was performed. As noted earlier, E (see Eq.(2)) is the selected measurement output after a time τ and E_r is the error made during the measurement of the energy, E . It is evident that maximization of the product τE_r ensures minimal disturbance associated with the measurement process. This product term is linked to the uncertainty principle, so that a lower limit τE_r would ensure maximal disturbance on the monitored system. A large error E_r and duration τ appear as key attributes of

a weak measurement. The finite duration τ yields a degree of uncertainty in energy of the observed quantum system. We therefore consider a weak non-Hermitian term, so that the system under observation evolves as $i\hbar\frac{\partial}{\partial t}|\psi(t)\rangle = H_{eff}|\psi(t)\rangle$. By expanding the state of the system within the unperturbed basis states $|n\rangle$ of the unmeasured system with Hamiltonian \hat{H}_0 as $|\psi(t)\rangle = \sum_n C_n(t)|n\rangle$, the coefficients $C_n(t)$ can be determined using the Schrödinger equation based on the Hamiltonian in Eq.(3).

The Hamiltonian \hat{H}_0 of the unmeasured qubit with energies E_1 (E_2) at state $|0\rangle$ ($|1\rangle$) is of the form

$$\hat{H}_0 = -\hbar\left(\frac{\Delta\omega}{2}\sigma_z + V(t)\sigma_x\right), \quad (4)$$

where the Pauli matrices $\sigma_x = |0\rangle\langle 1| + |1\rangle\langle 0|$, $\sigma_z = |1\rangle\langle 1| - |0\rangle\langle 0|$, $\Delta\omega = 2(E_1 + E_2)$ and the potential $V(t)$ which induces transitions between the two levels. The perturbation potential terms are taken to be $V_{00} = V_{11} = 0$ and $V_{01} = V_{10}^* = V_0 e^{i\omega(t-t_0)}$ with V_0 as a real number. The state of the measured system, $|\psi(t)\rangle$ evolves as³⁰

$$|\psi(t)\rangle = e^{-i(E_1 - i\lambda_1/4)t}C_1(t)|0\rangle + e^{-i(E_2 - i\lambda_2/4)t}C_2(t)|1\rangle \quad (5)$$

where $\lambda_1 = \frac{(E_1 - E)^2}{2\tau E_r^2}$ and $\lambda_2 = \frac{(E_2 - E)^2}{2\tau E_r^2}$ for a renormalized E_r .

The coefficients $C_1(t)$, $C_2(t)$ in Eq.(5) are obtained using³⁰

$$\begin{bmatrix} C_1(t) \\ C_2(t) \end{bmatrix} = \begin{bmatrix} \cos \kappa t - i\alpha_1 & -i\alpha_2 \\ -i\alpha_2 & \cos \kappa t + i\alpha_1 \end{bmatrix} \begin{bmatrix} C_1(0) \\ C_2(0) \end{bmatrix}, \quad (6)$$

where $\alpha_1 = \cos \theta \sin \kappa t$, $\alpha_2 = \sin \theta \sin \kappa t$, $\cos \theta = \frac{q}{\kappa}$, $\kappa = \sqrt{q^2 + V_0^2}$, $q = \frac{1}{2}(\omega - \Delta E + i\Omega/2)$, $\Delta E = (E_2 - E_1)$, and $\Omega = \lambda_2 - \lambda_1$. The qubit states of the monitored system therefore incorporate non-Hermitian terms which are functions of the measurement attributes

$$\begin{aligned} |\chi_s(t)\rangle &= e^{-\lambda_t t/4} (\cos \kappa t - i \cos \theta \sin \kappa t) |0\rangle \\ &\quad - i e^{-\lambda_t t/4} \sin \theta \sin \kappa t |1\rangle \\ |\chi_a(t)\rangle &= e^{-\lambda_t t/4} (\cos \kappa t + i \cos \theta \sin \kappa t) |1\rangle \\ &\quad - i e^{-\lambda_t t/4} \sin \theta \sin \kappa t |0\rangle, \end{aligned} \quad (7)$$

where $\lambda_t = \frac{\Delta E^2}{2\tau E_r^2}$. For measurement procedures which introduce very large errors, $E_r \rightarrow \infty$, $\lambda_1 = \lambda_2 = \lambda_t = \cos \theta = 0$, and the qubit oscillates coherently between the two levels with the Rabi frequency $2\kappa = 2V_0$ as is well known in the unmeasured system.

For a system in which the initial state at $t = 0$ is $|1\rangle$ and the final state at time t is either $|1\rangle$ or $|0\rangle$, the probability P_{11} (P_{10}) of the system to be in the state $|1\rangle$ ($|0\rangle$) depends on the relation between V_0 and λ_t . At the resonance frequencies, $\omega = \Delta E$, the Rabi frequency $2\kappa_0 = (4V_0^2 - (\frac{\lambda_t}{2})^2)^{1/2}$, and $\cos \theta = -i\lambda_t/4\kappa_0$. There exists two tunneling regimes with $V_0 > \frac{\lambda_t}{4}$ ($V_0 < \frac{\lambda_t}{4}$) applicable to the coherent (incoherent) cases. For the coherent tunneling regime we obtain³⁰

$$P_{11} = e^{-\lambda_t t/2} \left[\cos \kappa_0 t - \frac{\lambda_t}{4\kappa_0} \sin \kappa_0 t \right]^2 \quad (8)$$

$$P_{10} = e^{-\lambda_t t/2} \frac{V_0^2}{\kappa_0^2} \sin^2 \kappa_0 t, \quad (9)$$

where $\lambda_t = \frac{(E_2 - E_1)^2}{2\tau E_r^2}$. The total probabilities, $P_{11} + P_{10} \leq 1$, the loss of normalization is dependent on the measurement precision, E_r as expected. For the system undergoing incoherent tunneling, we replace $\sin[x]$ ($\cos[x]$) by $\sinh[x]$ ($\cosh[x]$). The dynamics at the exceptional point occurs at $\kappa_0 = 0$, $V_0 = \frac{\lambda_t}{4}$, and both regimes merge to a point in topological space. The two-level system can be seen as a non-ideal dissipative quantum system due to its coupling to a multitude of decay states associated with the measurement process.

III. CLASSICAL CORRELATION AND QUANTUM DISCORD

Following the formulation of quantum discord in Refs.¹³⁻¹⁵, we express the quantum mutual information of a composite state ρ of two subsystems A and B as $\mathcal{I}(\rho) = S(\rho_A) + S(\rho_B) - S(\rho)$ for a density operator in $\mathcal{H}_A \otimes \mathcal{H}_B$. ρ_A

(ρ_B) is the reduced density matrix associated with A (B) and $S(\rho_i)$ ($i=A,B$) denotes the well known von Neumann entropy of the density operator ρ_i , where $S(\rho) = -\text{tr}(\rho \log \rho)$. The mutual information can also be written in terms of quantum conditional entropy $S(\rho|\rho_A) = S(\rho) - S(\rho_A)$ as

$$\mathcal{I}(\rho) = S(\rho_B) - S(\rho|\rho_A) \quad (10)$$

A series of one-dimensional orthogonal projectors $\{\Pi_k\}$ induced in \mathcal{H}_A results in different outcomes of the measurement in \mathcal{H}_B via the post measurement conditional state

$$\rho_{B|k} = \frac{1}{p_k}(\Pi_k \otimes \mathbb{I}_B)\rho(\Pi_k \otimes \mathbb{I}_B) \quad (11)$$

where the probability $p_k = \text{tr}[\rho(\Pi_k \otimes \mathbb{I}_B)]$ and $\{\Pi_k\}$ denote the one-dimensional projector indexed by the outcome k . From the cumulative effect of the mutually exclusive measurements on A , we obtain a conditional entropy of the subsystem B based on $\rho_{B|k}$

$$S(\rho|\{\Pi_k\}) = \sum_k p_k S(\rho_{B|k}) \quad (12)$$

which is used to obtain the measurement induced mutual information $\mathcal{I}(\rho|\{\Pi_k\}) = S(\rho_B) - S(\rho|\{\Pi_k\})$. The classical correlation measure based on optimal measurements made on A is obtained as¹³⁻¹⁵

$$\mathcal{C}_A(\rho) = \sup_{\{\Pi_k\}} \mathcal{I}(\rho|\{\Pi_k\}) \quad (13)$$

The difference in $\mathcal{I}(\rho)$ and $\mathcal{C}_A(\rho)$ yields the non symmetric quantum discord $\mathcal{D}_A(\rho) = \mathcal{I}(\rho) - \mathcal{C}_A(\rho)$. The discord $\mathcal{D}_B(\rho)$ associated with measurements on subsystem B can be evaluated likewise. In general $\mathcal{D}_A(\rho) \neq \mathcal{D}_B(\rho)$. Measurements made on a neighboring partition hold the key to determining the classical correlation measure between the subsystems.

A. A qubit pair immersed in a common reservoir

The joint evolution of a pair of two-level qubit subsystems, A, B undergoing decoherence in a common reservoir is determined by a completely positive trace preserving map expressed in the operator-sum form⁴⁰⁻⁴²

$$\varepsilon(\rho_{AB}) = \sum_{i,j} \Gamma_i(A) \Gamma_j(B) \rho_{AB} \Gamma_i^\dagger(B) \Gamma_j^\dagger(A), \quad (14)$$

where $\Gamma_i(A)$ ($\Gamma_i(B)$) is the Kraus operator associated with the decoherence process at A (B). For the phase flip channel in which there is loss of quantum information with conservation of energy, the Kraus operators are given in the basis $\{|0\rangle, |1\rangle\}$ for both subsystems, $k = A, B$ as^{18,40} $\Gamma_0(A) = \text{diag}(\sqrt{1-p/2}, \sqrt{1-p/2}) \otimes \mathbf{1}_B$, $\Gamma_1(A) = \text{diag}(\sqrt{p/2}, -\sqrt{p/2}) \otimes \mathbf{1}_B$, $\Gamma_0(B) = \mathbf{1}_A \otimes \text{diag}(\sqrt{1-p/2}, \sqrt{1-p/2})$ and $\Gamma_1(B) = \mathbf{1}_A \otimes \text{diag}(\sqrt{p/2}, -\sqrt{p/2})$. The parameter $p = 1 - \exp(-\gamma t)$, where γ denotes the phase damping rate.

To simplify the numerical analysis, we consider a joint state of the pair of two-level qubit subsystems, A, B in an initial X -type state with maximally mixed marginals ($\rho_{A(B)} = I_{A(B)}/2$, $S(\rho_A(t)) = S(\rho_B(t)) = 1$). The density matrix appears in the form $\rho(0) = \frac{1}{4}[I + \sum_{i=1..3} c_i \sigma_A^i \otimes \sigma_B^i]$, where I is the identity operator associated with the qubit pair, σ_A^i , and σ_B^i , and σ_j^i ($j = A, B$, $i = 1, 2, 3$) are the Pauli operators of each qubit. c_i ($0 \leq |c_i| \leq 1$) are real numbers, with the Werner states sharing a common $|c_1| = |c_2| = |c_3| = c$ and $c=1$ for the Bell basis states. We assume that the usual unit trace and positivity conditions of the density operator ρ are satisfied. For the class of states where $|c_1| = |c_2| = c$, $|c_3| = c_3$, the evolution of the joint system is described by the matrix

$$\rho_{A,B}(t) = \frac{1}{4} \begin{pmatrix} 1+c_3 & 0 & 0 & 0 \\ 0 & 1-c_3 & 2ce^{\mu^*t} & 0 \\ 0 & 2ce^{\mu t} & 1-c_3 & 0 \\ 0 & 0 & 0 & 1+c_3 \end{pmatrix}, \quad (15)$$

where $\mu = [-2\gamma - i(\Delta\omega_A - \Delta\omega_B)]t$, and as noted earlier γ is the phase damping rate. To simplify the analysis, we have considered the same damping rate for the two qubit subsystems. $\Delta\omega_i$, $i = A, B$ denotes the difference in energy levels of each qubit subsystem, we consider equivalent energy levels in the qubit pair. The mutual information of state $\rho_{A,B}$ in Eq. (15) is evaluated using $\mathcal{I}(\rho_A : \rho_B) = 2 + \sum_{i=1}^4 \lambda_i \log \lambda_i$ where the eigenvalues λ_i of $\rho_{A,B}$ are $\lambda_{1,2} = \frac{1}{4}(1+c_3)$, $\lambda_3 = \frac{1}{4}(1-c_3+2ce^{-2\gamma t})$ and $\lambda_4 = \frac{1}{4}(1-c_3-2ce^{-2\gamma t})$

B. Influence of c_3 and c in the violation of a Bell inequality

The violation of the CHSH-Bell inequality function \mathcal{B} quantifies quantum nonlocal correlations which cannot be created by classical means^{43,44}. The CHSH inequality Bell function \mathcal{B} is $|\mathcal{B}| \leq 2$, where $\mathcal{B} = M(\vec{a}, \vec{b}) - M(\vec{a}, \vec{b}') + M(\vec{a}', \vec{b}) + M(\vec{a}', \vec{b}')$, where $M(\vec{a}, \vec{b})$ is the correlated results (± 1) arising from the measurement of two qubits in directions \vec{a} and \vec{b} . The CHSH-Bell inequality is violated when \mathcal{B} exceeds 2, and the correlations is considered inaccessible by any classical means of information transfer, while for values less than 2, the local hidden-variable theory satisfies the CHSH-Bell inequality.

We first investigate the influence of parameters $c_1 = c_2 = c$ and c_3 in a possible violation of the CHSH-Bell inequality. These results will be compared with the effect of c and c_3 on classical and quantum correlations in the next Section. For the density matrix in Eq. (15), \mathcal{B} based on correlations averages, is obtained using the following relations⁴⁵

$$\begin{aligned}\mathcal{B}(t, c, c_3) &= \text{Max} \{ \mathcal{B}_1(t, c, c_3), \mathcal{B}_2(t, c, c_3) \} \\ \mathcal{B}_1(t, c, c_3) &= 2\sqrt{e^{-4gt}c^2 + c_3^2} \\ \mathcal{B}_2(t, c, c_3) &= 2\sqrt{2}ce^{-2gt}\end{aligned}\tag{16}$$

In general, the interplay of several parameters (c, c_3, t, g) makes it a complex problem to examine the non-locality of the two-qubit density matrix, $\rho_{A,B}$. To simplify the approach, we note that the eigenvalues λ_i of $\rho_{A,B}$ in Eq. (15) need to satisfy the positivity criteria of assuming only non-negative values. To this end, $\lambda_4 = \frac{1}{4}(1 - c_3 - 2ce^{-2\gamma t})$ is most susceptible to violating this criteria when $c_3^m = 1 - 2ce^{-2\gamma t}$. Figure 1a,b show values of $\mathcal{B}(t, c, c_3)$ as a function of c, t , at two damping rates g , with $c_3 = c_3^m$. The results indicate that with increasing c , the system is likely to violate the Bell inequality during the initial period of measurement. There are subtle differences in the system non-locality arising from use of low and high g as can be inferred from Eq. (16). In Figure 1c where c_3 is not constrained, the system best exhibits classical features at low $c \approx 0.1$ and $c_3 \sim c$. There is a gradual shift towards possible violation of the CHSH-Bell inequality as c is increased, and when λ_4 becomes negative.

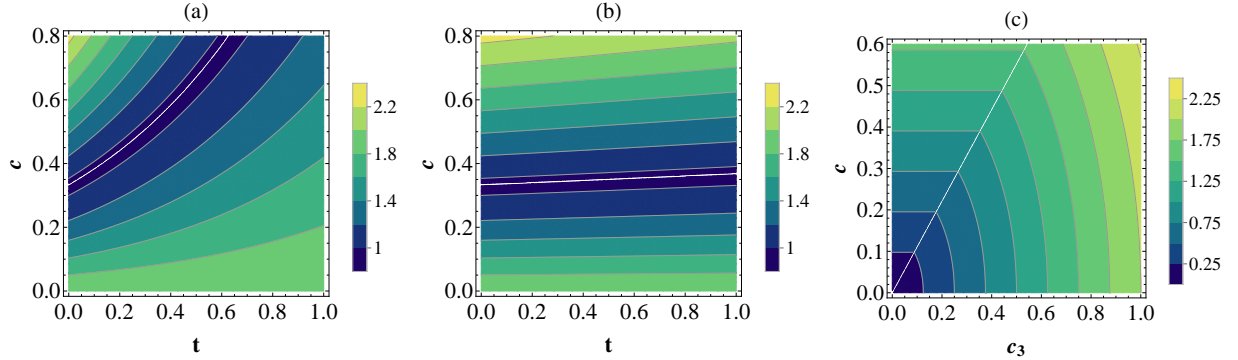


FIG. 1: (a) Bell inequality, \mathcal{B} (Eq. (16)) as function of unitless t/τ ($0 < t < \tau$) and c . c_3 is fixed at $c_3 = 1 - 2ce^{-2\gamma t}$. The measurement time duration, $\tau = 2\pi/V_0=1$, $c = 0.15$, and phase damping rate $g = \gamma\tau=0.7$. (b) All same except $g = \gamma\tau=0.05$. (c) Bell inequality, \mathcal{B} (Eq. (16)) as function of c and c_3 , $t=\tau$.

IV. MEASUREMENT PRECISION AND QUANTUM CORRELATIONS

The classical correlation measure is obtained through all possible local measurements on one of the subsystems, say A. For the ideal case of a local measurement that is instantaneous, we utilize a set of orthogonal projectors $\{\Pi_k = |\theta_k\rangle\langle\theta_k|, k = \parallel, \perp\}$, which are defined in terms of the orthogonal states

$$\begin{aligned}|\theta_{\parallel}\rangle &= \cos\theta|0\rangle + e^{i\phi}\sin\theta|1\rangle, \\ |\theta_{\perp}\rangle &= e^{-i\phi}\sin\theta|0\rangle - \cos\theta|1\rangle,\end{aligned}\tag{17}$$

where $0 \leq \theta \leq \pi/2$ and $0 \leq \phi \leq 2\pi$. In a recent work, Galve et. al.⁴⁶ showed that orthogonal measurements are sufficient to evaluate the quantum discord pertaining to rank 2 states of two qubit systems, but provide tight upper bounds for higher rank (3 and 4) states.

Using Eq. (7) as a basis, we modify the projection operators in Eq. (17) using generalized projectors that incorporate measurement attributes

$$\begin{aligned} |\theta_{\parallel}\rangle_p &= R(\theta) |0\rangle + e^{i\phi} S(\theta) |1\rangle, \\ |\theta_{\perp}\rangle_p &= e^{-i\phi} S(\theta) |0\rangle - R(\theta) |1\rangle, \end{aligned} \quad (18)$$

The terms $R(\theta) = e^{-\lambda_r t/4} (\cos \theta - i \frac{\lambda_r t}{4\theta} \sin \theta)$ and $S(\theta) = e^{-\lambda_r t/4} \frac{\sqrt{\theta^2 + (\lambda_r t/4)^2}}{\theta} \sin \theta$ with $\lambda_r = \frac{\Delta E^2}{2\tau E_r^2}$, ΔE being the energy difference between the $|1\rangle$ and $|0\rangle$ states of the qubit. In the limit of $\lambda_r \rightarrow 0$, Eq. (18) reverts back to the orthogonal set in Eq. (17). It is implicit that the orthogonal measurement projections in Eq. (18) may be in a state of evolution during the measurement process.

The generalized measurements as specified by the constituent maps in Eq. (18) can be projected as follows

$$\begin{aligned} & \frac{1}{2} |\theta_{\parallel}\rangle_p \langle \theta_{\parallel}|_p + \frac{1}{2} |\theta_{\perp}\rangle_p \langle \theta_{\perp}|_p, \\ &= \begin{pmatrix} |R(\theta)|^2 + |S(\theta)|^2 & 0 \\ 0 & |R(\theta)|^2 + |S(\theta)|^2 \end{pmatrix}, \\ &= \begin{pmatrix} 1 & 0 \\ 0 & 1 \end{pmatrix}, \quad \tau = \lambda_r = 0 \end{aligned} \quad (19)$$

The incorporation of measurement attributes (τ, p) therefore leads to non-preservation of the trace of the density matrix in Eq. (19). This can be attributed to loss of the particle from the system due to the observational mapping process. The dependence of the projected states given in Eq. (18) on the measurement attributes, τ and λ_r , results in the dependence of the classical correlation on these same attributes which we examine next.

The reduced density matrices, $\rho_B^{(k)}$ of the neighboring subsystem B in accordance with the two projective measurements ($p_{\parallel} = p_{\perp} = 1/2$) in subsystem A are obtained as

$$\rho_B^{\parallel} = \begin{pmatrix} \frac{1}{2}(1 - c_3 e^{-pt/2} [\varphi_1 - \varphi_2]) & \frac{1}{2} c e^{-2gt} \varphi_1 \varphi_2 \\ \frac{1}{2} c e^{-2gt} \varphi_1 \varphi_2 & \frac{1}{2}(1 + c_3 e^{-pt/2} [\varphi_1 - \varphi_2]) \end{pmatrix}, \quad (20)$$

$$\rho_B^{\perp} = \begin{pmatrix} \frac{1}{2}(1 + c_3 e^{-pt/2} [\varphi_1 - \varphi_2]) & -\frac{1}{2} c e^{-2gt} \varphi_1 \varphi_2 \\ -\frac{1}{2} c e^{-2gt} \varphi_1 \varphi_2 & \frac{1}{2}(1 - c_3 e^{-pt/2} [\varphi_1 - \varphi_2]) \end{pmatrix}. \quad (21)$$

where $\varphi_1 = \cos^2 \theta - (\frac{pt}{4\theta})^2 \sin^2 \theta - \frac{\xi^2}{\theta^2} \sin^2 \theta$, $\varphi_2 = \frac{\xi^2}{\theta^2} \sin^2 \theta$ and $\xi = \sqrt{\theta^2 + (pt/4)^2}$. $g = \gamma\tau$, the dimensionless time, t is obtained via division with the measurement duration, $\tau = 2\pi/V_0$ and the dimensionless precision parameter, $p = \lambda_r \tau$. The eigenvalues of the two reduced density matrices, $\rho_B^{(k)}$ of the neighboring subsystem B are obtained as

$$\begin{aligned} \zeta_{1,2}^{(k)} &= \frac{1}{2}(1 \pm \Theta), \\ \Theta^2 &= c_3^2 e^{-pt} [\varphi_1 - \varphi_2]^2 + 4c^2 e^{-4gt} e^{-pt} \varphi_1 \varphi_2 \end{aligned} \quad (22)$$

Using Eq. (22), we obtain $S(\rho_B^{\parallel}) = S(\rho_B^{\perp}) = -\text{tr}(\rho \log \rho) = -\frac{1-\Theta}{2} \log_2 \left[\frac{1-\Theta}{2} \right] - \frac{1+\Theta}{2} \log_2 \left[\frac{1+\Theta}{2} \right]$. The classical correlation given in Eq. (13) is evaluated using

$$\mathcal{C}(\rho) = 1 - \min_{\theta, \phi} R(\Theta), \quad (23)$$

Further evaluation of $\mathcal{C}(\rho)$ is simplified by the elimination of the parameter ϕ due to the choice of similar parameters, $|c_1| = |c_2| = c$. The maximal value of Θ is dependent on c_3, c, γ , the precision parameter p , and the measurement duration τ . It is obvious from Eq. (22), that the influence of the phase damping rate becomes pronounced at $c > c_3$.

The quantum discord is evaluated using

$$\mathcal{D}(\rho) = 2 + \sum_{k=1}^4 \lambda_k \log_2 \lambda_k - \mathcal{C}(\rho), \quad (24)$$

Figures 2, 3 highlight changes in the classical correlation \mathcal{C} and quantum discord \mathcal{D} as function of t ($0 < t < \tau$), based on numerical evaluation of Eqs. (22), (23), (24) and the eigenvalues λ_i of $\rho_{A,B}$ in Eq. (15). \mathcal{C} and \mathcal{D} undergo noticeable changes due to finite-time measurements on a neighboring partition at non-zero p , for input parameters $c_3 > c$. Figures 2b and 3b show that the quantum discord \mathcal{D} is enhanced, with a corresponding decrease in \mathcal{C} as p

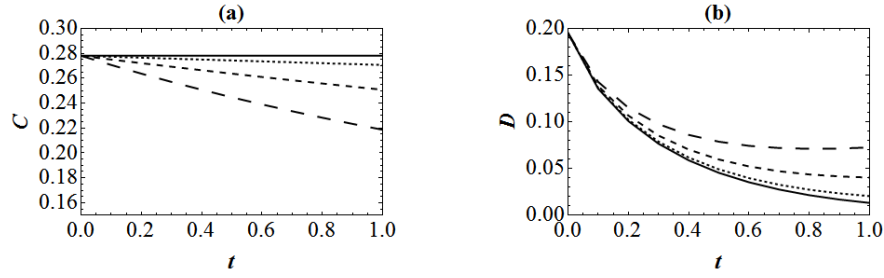


FIG. 2: (a) Classical correlation \mathcal{C} as function of t ($0 < t < \tau$) for various values of the measurement precision p . τ the measurement time duration is set at 1 and $g = \gamma\tau = 0.6$, where γ is the phase damping rate. The real numbers $c_1 = c_2 = c = 0.2$ and $c_3 = 0.6$. The curves from top to bottom correspond to the unitless measurement precision, $p = 0, 0.05, 0.2, 0.5$. and (b) Quantum discord \mathcal{D} as function of t ($0 < t < \tau$) for various values of the measurement precision $p = 0.5, 0.2, 0.05, 0$ (top to bottom). All other parameters are the same as in (a).

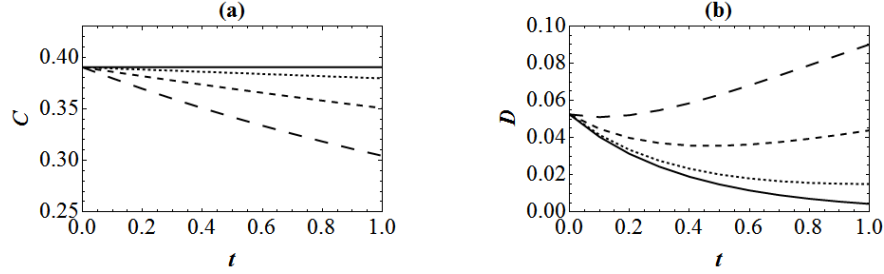


FIG. 3: a) Classical correlation \mathcal{C} as function of t ($0 < t < \tau$) for various values of the measurement precision p . τ the measurement time duration is set at 1 and $g = \gamma\tau = 0.6$. The real numbers $c_1 = c_2 = c = 0.1$ and $c_3 = 0.7$. The curves from top to bottom correspond to the unitless measurement precision, $p = 0, 0.05, 0.2, 0.5$. and (b) Quantum discord \mathcal{D} as function of t for various values of the measurement precision $p = 0.5, 0.2, 0.05, 0$ (top to bottom). All other parameters are the same as in (a).

is increased. The enhancement in the quantum discord \mathcal{D} is pronounced at a higher ratio $\frac{c_3}{c}$. However at $c > c_3$, the numerically evaluated classical correlation was noted to be almost insignificant, $\mathcal{C} \approx 0.01$ and \mathcal{D} was seen to be independent of p . These results indicate a trend towards more non-classical behaviour at increased p for the case when $c_3 > c$, however it is not immediately clear why a low \mathcal{C} is obtained at $c_3 < c$. Figures 4 and 5 illustrate the changes in \mathcal{C} and \mathcal{D} due to the dephasing rate g for various values of the measurement precision p . At $c < c_3$, the classical correlation \mathcal{C} remains independent of g , a trend that appears only beyond a critical g at $c > c_3$. This has also been noted in earlier works^{18,19} for the specific case, $p = 0$. Imperfect measurements carried out on the subsystem A therefore enhance the non-classical correlations of the adjacent subsystem B at $c_3 > c$.

It is not immediately clear as to the influence of quantum measurements in the region where $c < c_3$, even though it appears that there is less impact of measurements. Further investigations are needed to confirm the role of the CHSH-Bell inequality, \mathcal{B} in relation to the c, c_3 parameters. For instance in Figure 1, it appears that states which exhibit greater classical features (at low c , $c_3 > c$), are more likely to have reduced \mathcal{C} and increased \mathcal{D} with measurements carried out in an adjacent subsystem. On the other hand, states which are close to CHSH-Bell inequality violation ($c > c_3$) seem less influenced by imprecise measurement procedures.

V. INFORMATION-MEASUREMENT PRECISION TRADE-OFF

The results in Section IV highlight the effect of disturbance on the classical and non-classical correlations of the adjacent reduced density matrix, $\rho_B^{(k)}$. This disturbance is quantified by the measurement precision p and finite time duration τ associated with the imperfect projective measurements (Eq. (18)) on subsystem A . In this Section, we examine the implications of these results on the “information-disturbance relationship” on subsystem B as a result of imperfect measurements on subsystem A . We note the two sources of uncertainty (p, τ) which give rise to a probabilistic distribution of the quantity being measured.

Two important measures will be used to examine the tradeoff between information gained due to quantum measurement and the disturbance caused during observation: fidelity and trace distance. The fidelity, F ⁴⁸ which quantifies

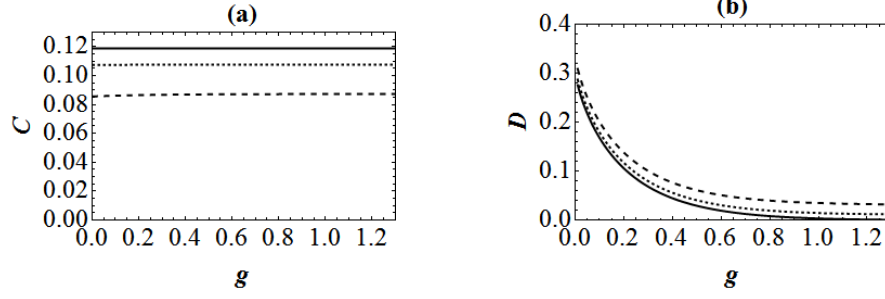


FIG. 4: (a) Classical correlation \mathcal{C} as function of the unitless $g = \gamma\tau$ where γ is the phase damping rate, for various values of the measurement precision p at $t=1$. The real numbers $c_1=c_2=c=0.3$ and $c_3=0.4$. The curves from top to bottom correspond to the unitless measurement precision, $p=0, 0.2, 0.7$. and (b) Quantum discord \mathcal{D} as function of g at $t=1$. for various values of the measurement precision $p=0.7, 0.2, 0$ (top to bottom). All other parameters are the same as in (a).

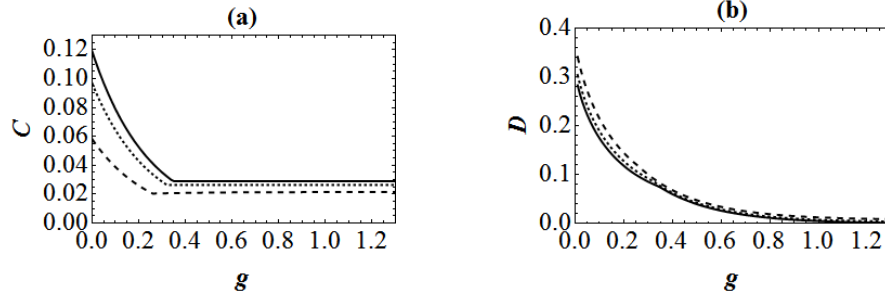


FIG. 5: (a) Classical correlation \mathcal{C} as function of the unitless $g = \gamma\tau$ where γ is the phase damping rate, for various values of the measurement precision p at $t=1$. The real numbers $c_1=c_2=c=0.4$ and $c_3=0.2$. The curves from top to bottom correspond to the unitless measurement precision, $p=0, 0.2, 0.7$. and (b) Quantum discord \mathcal{D} as function of g at $t=1$ at measurement precision $p=0.7, 0.2, 0$ (top to bottom). All other parameters are the same as in (a).

the distance between two states appear as

$$F[\rho_1, \rho_2] = \left\{ \text{Tr} \left[\sqrt{\sqrt{\rho_1} \rho_2 \sqrt{\rho_1}} \right] \right\}^2, \quad (25)$$

and is bounded by $0 \leq F[\rho_1, \rho_2] \leq 1$. The measurement disturbance on the dynamics of a system can be quantified using²³

$$D_i = 1 - F[\rho_1, \rho_2] \quad (26)$$

Based on the reduced density matrices $\rho_B^\parallel(t=0, p=0)$ and $\rho_B^\parallel(t, p)$ (Eq. (20)), the disturbance, D_i can be evaluated as a function of t and p .

To quantify the information gained from the system, we define the uncertainty $H(\nu)$ based on the parameter ν where

$$\nu = \frac{1}{2} - \frac{1}{2} T_d(\rho_1, \rho_2) \quad (27)$$

The trace distance, T_d between density matrices, ρ_1, ρ_2 , is given by half of the trace norm of the difference of the matrices as $T_d(\rho_1, \rho_2) = \frac{1}{2} \text{Tr}[\|\rho_1 - \rho_2\|]$ and $H(x) = -x \log_2 x - (1-x) \log_2 (1-x)$. In order to analyse the influence of the precision p and t , we consider $\rho_1 = \rho_B^\parallel(t=0, p=0)$ and $\rho_2 = \rho_B^\parallel(t, p)$. We next investigate the information-disturbance tradeoff relation²³

$$1 - F[\rho_1, \rho_2] \geq 1 - H[\nu(p, t)] \quad (28)$$

where the mutual information $(1-H[\nu(p, t)])$ is evaluated based on ν (Eq. (27)) for given values of the measurement attributes, p, t . Eq. (28) specifies that the disturbance between two states ρ_1, ρ_2 has a lower bound, quantified by the gain in information due to measurements. An alternative interpretation of Eq. (28) was also provided²³ through

the existence of a lower limit to the sum of the disturbance $1 - F$ and the uncertainty $H[\nu(p, t)]$ that is based on verification of the difference in the two states, ρ_1, ρ_2 . The difference between disturbance, $D_i (\times 100\%)$ and gain in information $(1 - H(\nu(p, t))) (\times 100\%)$ as a function of t and precision p is shown in Figure 6a,b. We note that for the input parameters ($c_1 = c_2 = c=0.4, c_3=0.1$), there exists a range of p and t for which the “information-disturbance relationship” (Eq. (28)) formulated in Ref.²³ is violated.

Comparing the results in Figure 6 a,b with those in Figures 2, 3, one notes that the appearance of increased quantum discord is invariably linked to the non-violation of the inequality in Eq. (28) when $c_3 > c$. The difference between the disturbance, D_i (Eq. (26)) and the mutual information $(1-H(\nu(p, t)))$ yields a measure of the quantum discord. This difference is accentuated at increasing p , a trend that is also observed in the enhancement of the quantum discord \mathcal{D} at higher p . One can expect a zero discord when the lower bound in Eq. (28) is reached, at which point the disturbance on the system equates the amount of information that can be retrieved. Another important observation relates to the case when $c > c_3$, where we earlier noted the existence of a small $\mathcal{C} \approx 0.01$ and \mathcal{D} that was immune to changes in p . Interestingly, we note that a violation of Eq. (28) occurs when $c > c_3$ and for a range of p, t as illustrated in Figure 6b.

One possible explanation of the noted violation may lie in the presence of other unseen neighboring subsystems which gives rise to a net deficit in quantum discord, as far as the two known subsystems A, B are concerned. This results in greater retrieval of information than the actual disturbance on the system, with bearings very similar to the Maxwell’s demon model⁴⁷. In the latter model, positive entropy production during measurement arise from work performed by other agents, ensuring that the second law of thermodynamics remains intact.

The results in Figure 6 a,b can partly be interpreted on the basis of earlier obtained results in Figure 1 a,b,c, where we noted that at higher $c > c_3$, there is trend towards violation of the CHSH-Bell inequality. The violation of Heisenberg’s “measurement-disturbance relationship” as evidenced by the nature of the c, c_3 input parameters, may have its origins in non-local quantum states which are also influenced by these same parameters. To this end, investigations involving rigorous mathematical formulations⁴⁹ of the underlying abstract Hilbert space are needed to provide greater insight to the links between the information-disturbance tradeoff relation, quantum discord and quantum non-locality based on the CHSH-Bell inequality function \mathcal{B} (Eq. (16)). The results obtained here may be useful in the interpretation of experimental results²⁸ showing similar violation of the “measurement-disturbance relationship”.

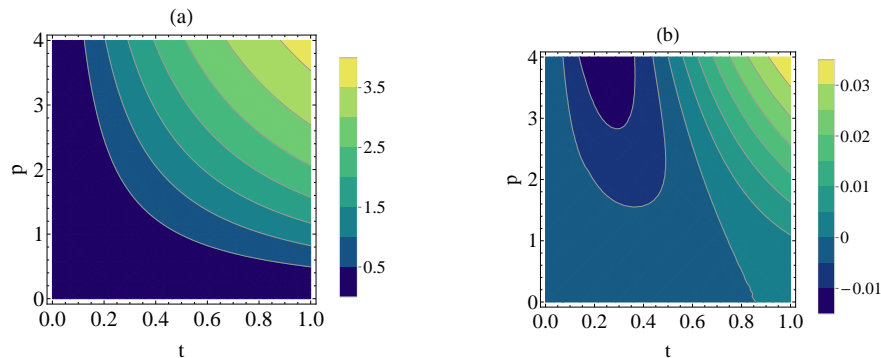


FIG. 6: (a) Contour-plots showing the trade-off between the measurement disturbance and information gain. Difference between disturbance, $D_i (\times 100\%)$ and gain in information $(1-H(\nu(p, t))) (\times 100\%)$ as a function of t and precision p . $\rho_1=\rho_B^\parallel(t=0, p=0)$ and $\rho_2=\rho_B^\parallel(t, p)$ (Eq. (20)). $c_1 = c_2 = c=0.1, c_3=0.7, g = \gamma\tau=0.5$ and $\theta=90$. (b) Description and parameters are the same as in (a) with the exception of $c_1 = c_2 = c=0.4, c_3=0.1$. A range of p and t for which the difference between disturbance, and gain in information is negative becomes noticeable.

VI. NON-MARKOVIANITY DURING QUANTUM MEASUREMENTS

To better understand the flow of information during quantum measurements, we consider the appearance of non-Markovianity, in relation to the attributes, p, t . Quantum systems undergoing Markovian dynamics observe a completely positive, trace preserving dynamical map $\Lambda(t), \rho(0) \rightarrow \rho(t) = \Lambda(t)\rho(0)$, which constitutes the one parameter semi-group obeying the composition law^{50–52}, $\Lambda(t_1)\Lambda(t_2) = \Lambda(t_1 + t_2)$, $t_1, t_2 \geq 0$. Accordingly, the fidelity function $F[\rho(t), \rho(t + \tau)]$ involving the initial state $\rho(t)$ and the evolved state $\rho(t + \tau)$ at a later time $t + \tau$, under Markovian

dynamics satisfies the inequality⁵¹

$$\begin{aligned} F[\rho(t), \rho(t+\tau)] &\equiv F[\Lambda(t)\rho(0), \Lambda(t)\rho(\tau)] \\ &\Rightarrow F[\rho(t), \rho(t+\tau)] \geq F[\rho(0), \rho(\tau)]. \end{aligned} \quad (29)$$

Any violation of this inequality is a signature of non-Markovian dynamics which can be observed via the fidelity difference function

$$\Delta(t, \tau) = \frac{F[\rho(t), \rho(t+\tau)] - F[\rho(0), \rho(\tau)]}{F[\rho(0), \rho(\tau)]}, \quad (30)$$

Negative values of $\Delta(t, \tau)$ serve as sufficient but not necessary condition of non-Markovianity. Using Eq. (30), we have evaluated the fidelity difference $G(t, \tau)$ as a function of t and θ for the density matrices corresponding to $\rho_1 = \rho_B^\parallel(t=0, p=0)$ and $\rho_2 = \rho_B^\parallel(t, p)$ (Eq. (20)), as illustrated in Figures 7 and 8. The figures highlight important differences between systems where $c_3 > c$ and those with $c > c_3$. In the regions midway: $25 < \theta < 42$, there is enhancement of non-Markovianity with precision p when $c_3 > c$. In systems where $c_3 < c$, the non-Markovian regions are located at the peripheral regions, $\theta \approx 0, 90$. We note that at $c_3 > c$ the optimized angle θ used in the evaluation of the classical correlation in Eq. (23) is about 90, decreasing gradually with increase p . At $c_3 < c$, the optimized angle $\theta < 30$. These results highlight the role of c, c_3 parameters in determining the links between non-Markovian dynamics and optimization processes associated with the classical correlation measure.

The findings in Figures 7 and 8 may provide a speculative basis to examine links between violation of the “measurement-disturbance relationship” in Eq. (28) and non-Markovianity. Is it possible that a pathway for violation of this relationship is attained when gain in information exceeds disturbance between two states via non-Markovian processes? This challenging question needs experimental verification using more generalized systems, as numerical results related to just two subsystems have been provided here.

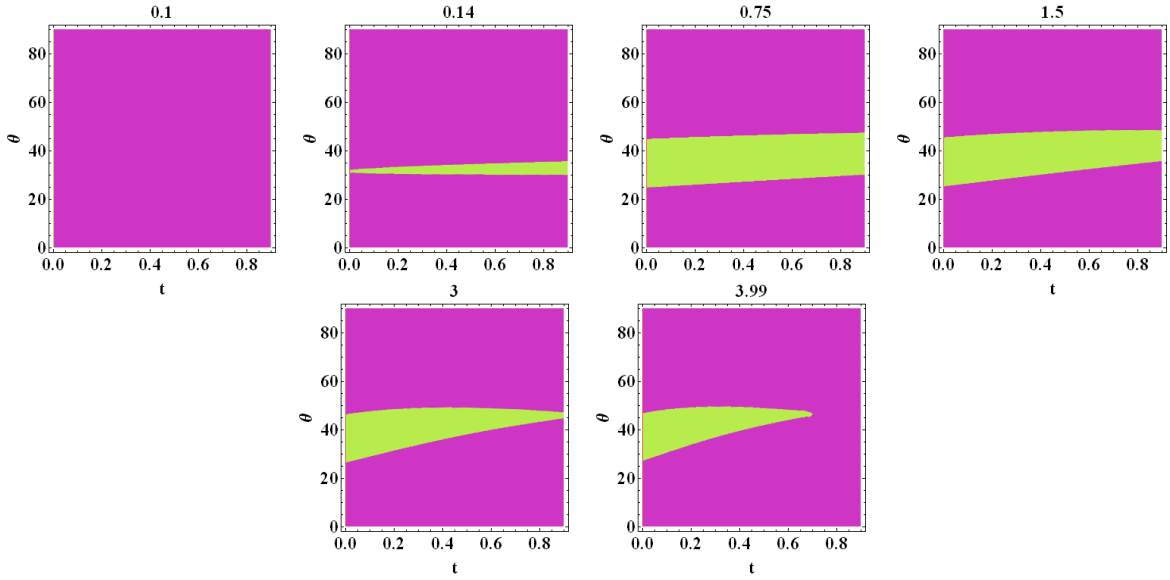


FIG. 7: Fidelity difference $\Delta(t, \tau)$ as a function of t and θ for the density matrices corresponding to $\rho_1 = \rho_B^\parallel(t=0, p=0)$ and $\rho_2 = \rho_B^\parallel(t, p)$ (Eq. (20)). We set $\tau=0.1$, $c_1 = c_2 = c=0.1$, $c_3=0.8$, $g = \gamma\tau=0.1$. Values of p are indicated at the top of each figure. Regions of negative values indicating non-Markovianity are shaded green show increase with precision p , and are dominant in the range $25 < \theta < 42$ deg.

VII. CONCLUSION

In conclusion, we have presented results of the influence of non-ideal attributes such as the measurement precision and finite measurement time duration on the classical correlation and quantum discord for a qubit pair immersed in a common environment. The results show that the quantum discord is enhanced as the precision of the measuring instrument is increased for a range of parameters, and both the classical correlation and the quantum discord undergo

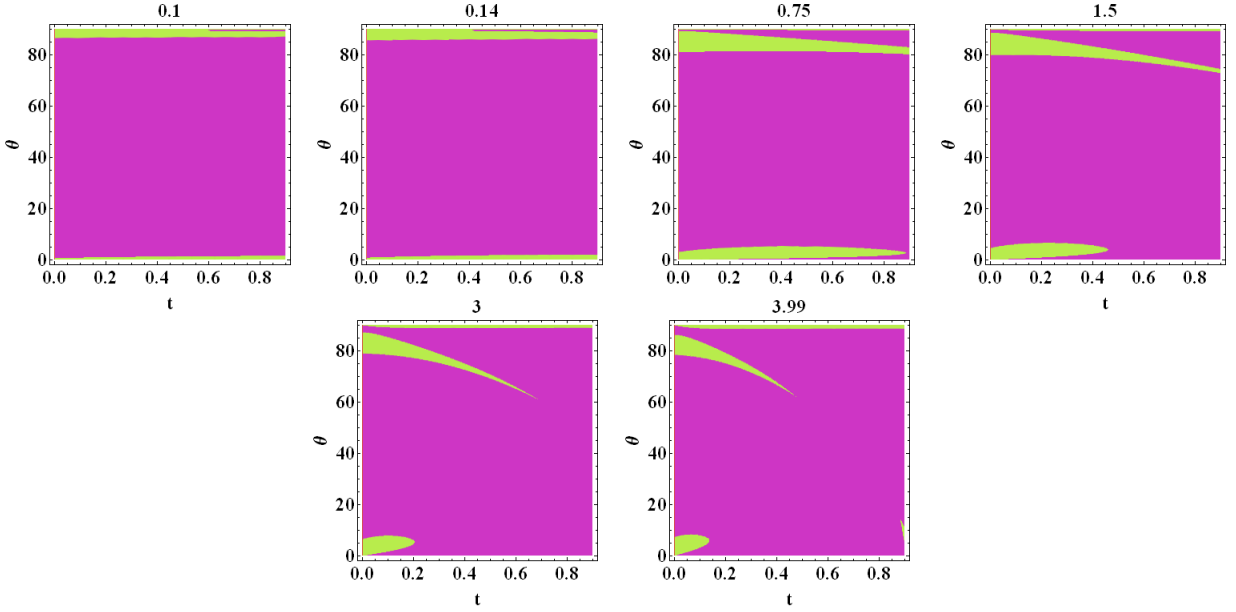


FIG. 8: Fidelity difference $\Delta(t, \tau)$ as a function of t and θ for the density matrices corresponding to $\rho_1 = \rho_B^\parallel(t=0, p=0)$ and $\rho_2 = \rho_B^\parallel(t, p)$ (Eq. (20)). We set $\tau=0.1$, $c_1 = c_2 = c=0.4$, $c_3=0.1$, $g = \gamma\tau=0.1$. Values of p are indicated at the top of each figure. Regions of negative values indicating non-Markovianity are shaded green and are located at the peripheral regions, $\theta \approx 0, 90$.

noticeable changes during the duration when measurements are performed on a neighboring partition. We also conclude that increased quantum discord within two subsystems, is invariably linked to the non-violation of the inequality associated with the “information-disturbance relationship”. We note that a zero discord corresponds to the lower bound in this inequality, consistent with the point at which the disturbance on the system equates the amount of information that can be retrieved. A violation of this inequality indicates a deficit in quantum discord, with the possibility that other undetected agents may be responsible in giving rise to a greater retrieval of information than the actual disturbance on the system. Overall, the results obtained in this work indicate that the fundamental limits of quantum mechanical measurements may be altered by exchanges involving non-classical correlations such as the quantum discord with external sources.

The violation of the “information-disturbance relationship” may have links with quantum non-locality and non-Markovian quantum dynamics of states that do not necessarily evolve via a completely positive, trace preserving dynamical maps. This study identifies (though not conclusively) that a possible pathway for violation of this relationship may occur when gain in information exceeds disturbances between two states via non-Markovian processes. Further scrutiny of the intricate links between these entities require mathematically rigorous approaches⁴⁹ and experimental verifications, however the results obtained in this study have wider implications for exploiting the subtleties of the Uncertainty Principle in multipartite systems. Cryptographic technologies specify that eavesdroppers can be detected as a result of disturbances caused by their measuring activities. The results obtained here indicates that eavesdroppers can remain undetected in some instances (when positivity of the density matrix of the observed system is violated). These ideas may be further extended to the development of sensitive quantum probes of fragile material systems, involving single atoms and molecules, and including living tissue matter.

Lastly, this study shows that the joint examination of several entities (non-locality, non-Markovianity, negative quantum discord) is needed in investigations involving quantum measurements of optics and nanostructure systems^{53,54}. The possibility that an analogous “information-disturbance relationship” may be violated in light-harvesting systems^{55–59} is an area for future investigation of systems which display exceptionally high efficiencies of energy transfer processes.

VIII. ACKNOWLEDGEMENTS

This research was undertaken on the NCI National Facility in Canberra, Australia, which is supported by the Australian Commonwealth Government. The author gratefully acknowledges the support of the Julian Schwinger

Foundation Grant, JSF-12-06-0000. The author would like to thank the anonymous referees for helpful comments.

-
- * Electronic address: thilaphys@gmail.com
- ¹ J. von Neumann, "Mathematical Foundations of Quantum Mechanics," Princeton University Press, Princeton, (1955).
 - ² Zeh, H. Dieter. "On the interpretation of measurement in quantum theory." *Foundations of Physics* **1**, no. 1 (1970): 69-76.
 - ³ Kofman, A. G. and Kurizki, G., "Acceleration of quantum decay processes by frequent observations." *Nature* **405**, no. 6786 (2000): 546-550.
 - ⁴ Misra, B., and Sudarshan, E. C. G., "The Zenos paradox in quantum theory", *Journal of Mathematical Physics*, **18**, 756, (1977).
 - ⁵ Facchi, P., and Pascazio, S., "Quantum Zeno dynamics: mathematical and physical aspects.", *Journal of Physics A: Mathematical and Theoretical* **41**, 493001 (2008); Facchi, P., and Pascazio, S., "Quantum zeno subspaces." *Phys. Rev. Lett.* **89**, 080401 (2002).
 - ⁶ Braginsky V. B. and Khalili F. Ya., "Quantum Measurement", K. S. Thorne editor (Cambridge University Press, Cambridge) (1992), and references cited therein.
 - ⁷ Mensky M. B., "Continuous Quantum Measurements and Path-Integrals" (Institute of Physics Publishers, Bristol and Philadelphia) (1993).
 - ⁸ Zurek, W. H., "Decoherence and the Transition from Quantum to Classical", *Phys. Today* **44** (10), 36 (1991).
 - ⁹ Zurek, W. H. "Environment-induced superselection rules.", *Phys. Rev. D* **26**, 1862 (1982).
 - ¹⁰ Schlosshauer, M., "Decoherence and the Quantum-to-Classical Transition", Springer-Verlag, (2008).
 - ¹¹ R. Ruskov and A. N. Korotkov,
Ruskov, R., and Korotkov, A. N., "Entanglement of solid-state qubits by measurement.", *Phys. Rev. B* **67**, 241305(R) (2003).
 - ¹² Englert B. G., "On quantum theory", arXiv:quant-ph:arXiv:1308.5290 (2013).
 - ¹³ Ollivier, H., and Zurek, W. H. , "Quantum discord: a measure of the quantumness of correlations.", *Phys. Rev. Lett.* **88**, 017901 (2001).
 - ¹⁴ Henderson, L., and Vedral, V., "Classical, quantum and total correlations.", *J. Phys. A* **34**, 6899 (2001).
 - ¹⁵ Vedral, V., "Classical correlations and entanglement in quantum measurements.", *Phys. Rev. Lett.* **90**, 050401 (2003).
 - ¹⁶ Coffman, V., Kundu, J., and Wootters, W. K., "Distributed entanglement.", *Phys. Rev. A* **61**, 052306 (2000).
 - ¹⁷ Brodutch, A., and Terno, D. R., "Quantum discord, local operations, and Maxwells demons.", *Rev. A* **81**, 062103 (2010).
 - ¹⁸ Maziero, J., Celeri, L. C., Serra, R. M., and Vedral, V., "Classical and quantum correlations under decoherence.", *Phys. Rev. A* **80**, 044102 (2009).
 - ¹⁹ Mazzola, L., Piilo, J., and Maniscalco, S., "Sudden transition between classical and quantum decoherence.", *Phys. Rev. Lett.* **104**, 200401 (2010).
 - ²⁰ Ciliberti, L., Rossignoli, R., and Canosa, N., "Quantum discord in finite XY chains.", *Phys. Rev. A* **82**, 042316 (2010).
 - ²¹ Datta, A., Shaji, A., and Caves, C. M., "Quantum discord and the power of one qubit.", *Phys. Rev. Lett.* **100**, 050502 (2008).
 - ²² Sacchi, M. F., "Information-Disturbance Tradeoff in Estimating a Maximally Entangled State.", *Phys. Rev. Lett.* **96**, 220502 (2006).
 - ²³ Maccone, L., "Information-disturbance tradeoff in quantum measurements", *Phys. Rev. A* **73**, 042307 (2006).
 - ²⁴ D'Ariano, G. M., "On the Heisenberg principle, namely on the information-disturbance trade-off in a quantum measurement.", *Fortschritte der Physik* **51**, 318-330(2003)
 - ²⁵ Buscemi, F., and Sacchi, M. F., "Information-disturbance trade-off in quantum-state discrimination.", *Phys. Rev. A* **74**, 052320 (2006).
 - ²⁶ Maccone, L., "Entropic information-disturbance tradeoff.", *EPL* **77**, 40002 (2007).
 - ²⁷ W. Heisenberg, *The physical principles of the Quantum Theory*, Dover (1930).
 - ²⁸ Rozema, L. A., Darabi, A., Mahler, D. H., Hayat, A., Soudagar, Y., and Steinberg, A. M., "Violation of Heisenbergs measurement-disturbance relationship by weak measurements.", *Phys. Rev. Lett.* **109**, 100404 (2012).
 - ²⁹ Wolfgramm, F., Vitelli, C., Beduini, F. A., Godbout, N., and Mitchell, M. W., "Entanglement-enhanced probing of a delicate material system.", *Nature Photonics* **7**, 28 (2013).
 - ³⁰ Thilagam, A., "Exceptional points and quantum correlations in precise measurements.", *J. Phys. A* **45**, 444031 (2012).
 - ³¹ R. P. Feynman and A. R. Hibbs, *Quantum Mechanics and Path Integrals*, (McGraw-Hill, New York) (1965).
 - ³² Feynman, R. P., "Space-time approach to non-relativistic quantum mechanics.", *Rev. Mod. Phys.* **20**, 367 (1948).
 - ³³ Mensky, M. B., "Quantum restrictions for continuous observation of an oscillator.", *Phys. Rev. D* **20**, 384 (1979); *Sov. Phys. JETP* **50**, 667 (1979).
 - ³⁴ Mensky, M. B., Onofrio, R., and Presilla, C., "Optimal monitoring of position in nonlinear quantum systems.", *Phys. Rev. Lett.* **70**, 2825 (1993).
 - ³⁵ Mensky, M. B., Onofrio, R., and Presilla, C., "Continuous quantum monitoring of position of nonlinear oscillators.", *Phys. Lett. A* **161**, 236-240 (1991).
 - ³⁶ Onofrio, R., Presilla, C., and Tambini, U., "Quantum Zeno effect with the Feynman-Mensky path-integral approach.", *Phys. Lett. A* **183**, 135-140 (1993).

- ³⁷ Tambini, U., Presilla, C., and Onofrio, R., “Dynamics of quantum collapse in energy measurements.”, *Phys. Rev. A* **51**, 967 (1995).
- ³⁸ Audretsch, J., and Mensky, M., “Continuous fuzzy measurement of energy for a two-level system.”, *Phys. Rev. A* **56**, 44 (1997).
- ³⁹ Heiss, W. D., “Repulsion of resonance states and exceptional points.”, *Phys. Rev. E* **61**, 929 (2000).
- ⁴⁰ Salles, A., de Melo, F., Almeida, M. P., Hor-Meyll, M., Walborn, S. P., Ribeiro, P. S., and Davidovich, L., “Experimental investigation of the dynamics of entanglement: Sudden death, complementarity, and continuous monitoring of the environment.”, *Phys. Rev. A* **78**, 022322 (2008).
- ⁴¹ E.C.G. Sudarshan, P.M. Mathews, J. Rau, “Stochastic Dynamics of Quantum-Mechanical Systems”, *Phys. Rev.* **121**, 920-924 (1961).
- ⁴² K. Kraus, “States, Effects, and Operations: Fundamental Notions of Quantum Theory”, Springer (1983)
- ⁴³ Bell, J. S., “On the einstein-podolsky-rosen paradox.”, *Physics* **1**, 195-200 (1964).
- ⁴⁴ Clauser, J. F., Horne, M. A., Shimony, A., and Holt, R. A., “Proposed experiment to test local hidden-variable theories”, *Phys. Rev. Lett.* **23**, 880-884 (1969).
- ⁴⁵ Bellomo, B., Franco, R. L., and Compagno, G., “Dynamics of non-classically-reproducible entanglement.”, *Phys. Rev. A* **78**, 062309 (2008).
- ⁴⁶ Galve, F., Giorgi, G. L., and Zambrini, R., “Orthogonal measurements are almost sufficient for quantum discord of two qubits.”, *EPL (Europhysics Letters)*, **96**, 40005 (2011).
- ⁴⁷ Szilard, L., “Über die Entropieverminderung in einem thermodynamischen System bei Eingriffen intelligenter Wesen.”, *Zeitschrift für Physik*, **53**(11-12), 840-856 (1929).
- ⁴⁸ Jozsa, R., “Fidelity for mixed quantum states.”, *Journal of Modern Optics*, **41** (12), 2315-2323 (1994).
- ⁴⁹ Anandan, J., and Aharonov, Y., “Geometry of quantum evolution.”, *Phys. Rev. Lett.* **65**, 1697 (1990).
- ⁵⁰ Wolf, M. M., Eisert, J., Cubitt, T. S., and Cirac, J. I., “Assessing non-Markovian quantum dynamics.”, *Phys. Rev. Lett.* **101**, 150402 (2008).
- ⁵¹ Rajagopal, A. K., Devi, A. U., and Rendell, R. W., “Kraus representation of quantum evolution and fidelity as manifestations of Markovian and non-Markovian forms.”, *Phys. Rev. A* **82**, 042107 (2010).
- ⁵² Breuer, H. P., Laine, E. M., and Piilo, J., “Measure for the degree of non-Markovian behavior of quantum processes in open systems”, *Phys. Rev. Lett.* **103**, 210401 (2009).
- ⁵³ Hall, M. A., Altepeter, J. B., and Kumar, P., “Drop-in compatible entanglement for optical-fiber networks”, *Optics Express*, **17**, 14558-14566 (2009).
- ⁵⁴ Tittel, W., Brendel, J., Zbinden, H., and Gisin, N., “Violation of Bell inequalities by photons more than 10 km apart”, *Phys. Rev. Lett.* **81**, 3563 (1998).
- ⁵⁵ Caruso, F., Chin, A. W., Datta, A., Huelga, S. F., and Plenio, M. B., “Highly efficient energy excitation transfer in light-harvesting complexes: The fundamental role of noise-assisted transport”, *J. Chem. Phys.* **131**, 105106-105106 (2009).
- ⁵⁶ Rebentrost, P., Mohseni, M., and Aspuru-Guzik, A., “Role of quantum coherence and environmental fluctuations in chromophoric energy transport”, *J. Phys. Chem. B* **113**, 9942-9947 (2009).
- ⁵⁷ Thilagam, A., “Non-Hermitian exciton dynamics in a photosynthetic unit system”, *J. Chem. Phys.* **136**, 065104 (2012); Thilagam, A., “Multipartite entanglement in the Fenna-Matthews-Olson (FMO) pigment-protein complex.”, *J. Chem. Phys.* **136**, 175104 (2012).
- ⁵⁸ Thilagam, A., and Usha Devi, A. R., “Non-Markovianity and Clauser-Horne-Shimony-Holt (CHSH)-Bell inequality violation in quantum dissipative systems”, *J. Chem. Phys.* **137**, 215103-215103 (2012).
- ⁵⁹ Caram, J. R., Lewis, N. H., Fidler, A. F., and Engel, G. S., “Signatures of correlated excitonic dynamics in two-dimensional spectroscopy of the Fenna-Matthew-Olson photosynthetic complex.”, *J. Chem. Phys.* **137**, 024507 (2012).